

# Characteristics of an impulse turbine

Hydraulics Laboratory  
Course: **ME39606**

Department of Mechanical Engineering  
Indian Institute of Technology, Kharagpur

## Objective

1. To determine the characteristic curve: unit power v/s unit speed.
2. To determine iso-efficiency curves.

## Procedure

1. Study the setup and make a line diagram.
2. Select a suitable head ( $H$ ).
3. Set the gate opening at 100%.
4. For a particular load on the turbine, note the rate of discharge, torque ( $\tau$ ), and the speed of the turbine ( $N$ ). Care should be taken to maintain a constant speed. The speed should be within the safe operating range (800-1800 rpm).
5. Repeat step 4 for different loads.
6. Repeat steps 4 and 5 for 75%, 50%, and 25% gate openings.

## Experimental observations

$$\text{Unit Power} = K_1 = P/H^{3/2}$$

$$\text{Unit Speed} = K_2 = N/\sqrt{H}$$

$$\text{Unit Discharge} = K_3 = Q/\sqrt{H}$$

[Exercise: Derive the above formulae]

Efficiency ( $\eta$ ) =  $P/(\rho Qgh) = N\tau/(\rho QgH)$ , here  $Q$  is found from the calibration curve (see below),  $g$  is the acceleration due to gravity

RPM (N) [/min]	Torque ( $\tau$ ) [Nm]	Power (P) [kW]	Unit Power ( $K_1$ )	Unit Speed ( $K_2$ )	$\eta$

## Characteristic diagram

The turbine is first tested for a particular gate opening; the speed and head are varied, and the discharge and brake horse-power are measured. From these results, values of the efficiency, unit power and unit speed are calculated for the various speeds and heads at that gate opening. A curve is then plotted for this gate opening with unit power and unit speed as ordinates; the efficiency for each point obtained is to be written on the curve at that point in the graph. These tests are repeated for various gate openings, and the efficiencies plotted as mentioned above. By examining the efficiencies written at each point, lines of equal efficiency can be drawn by interpolation; these lines correspond to the *iso-efficiency curves*. From this chart it can be seen at a glance what the speed of the turbine should be, for any gate opening. The chart also shows clearly the maximum efficiency of the turbine for given conditions, and the values of the gate opening and speed which produce this maximum efficiency can be read off the chart (this would ideally be the normal operating condition of the turbine). Please note that plotting unit power and unit speed, instead of the actual power and speed, has reduced all the results to unit head; thus, variation of the head is eliminated.

**Calibration curve for 6" venturimeter:** Use the following empirical relation for  $\Delta H$  beyond 140mm of Hg  $\Rightarrow Q \left[ \frac{m^3}{hr} \right] = 70.2584 - 0.0497 (\Delta H) + 0.0014 (\Delta H)^2$

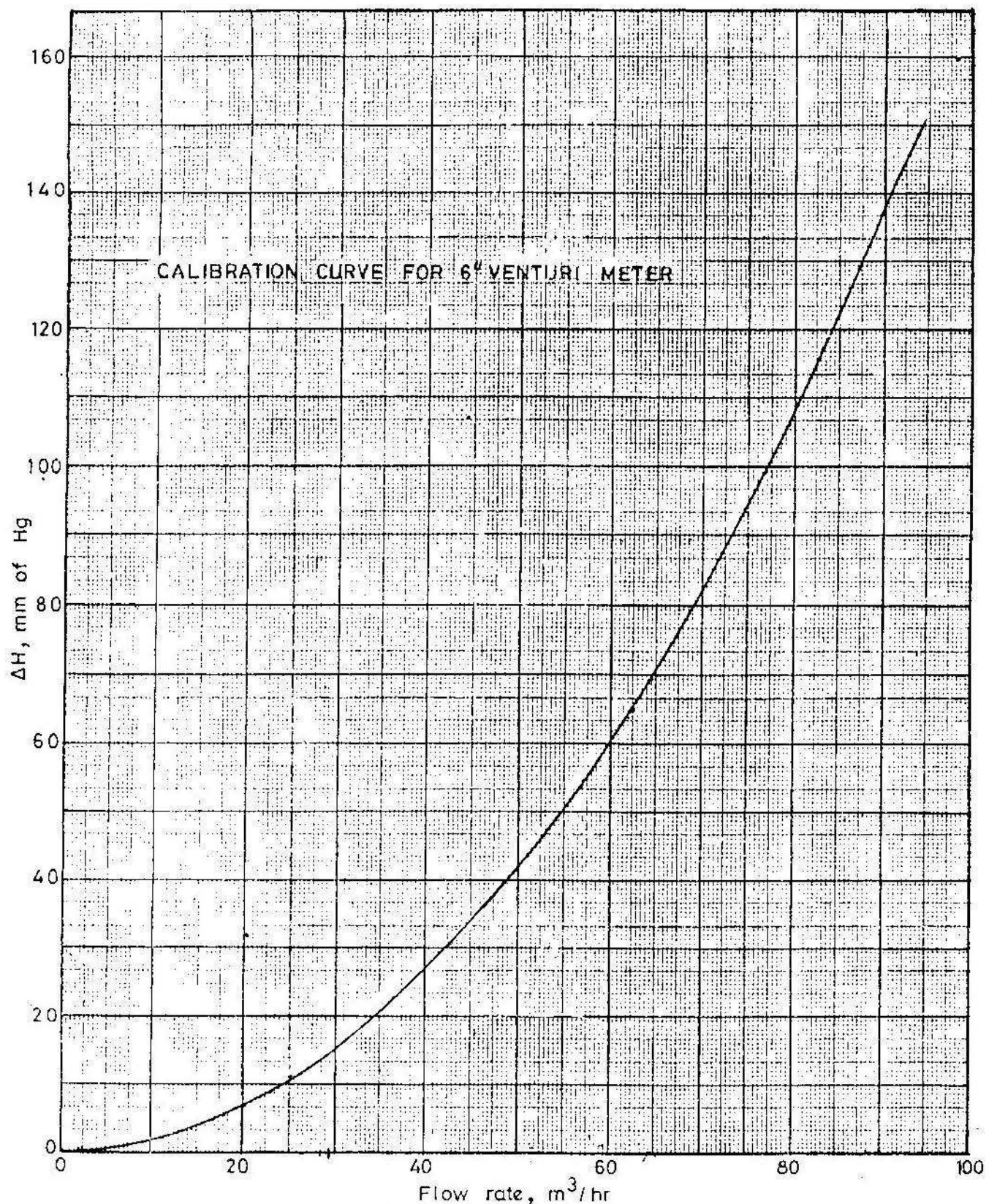


**Fig. 1: Schematic of main setup**



1. Display readings
2. Strain gauge
3. Friction-type hydraulic dynamometer
4. Handles to apply and reduce load
5. Pressure gauge at the inlet of the turbine
6. Valve at the inlet of the turbine
7. Impulse turbine
8. U-tube manometer
9. Tachometer

Fig. 2: Setup to provide high head of water



1. Electric motor
2. Main centrifugal pump for supply of high head of water to impulse turbine
3. Small centrifugal pump for priming the main centrifugal pump
4. Pressure gauge
5. Control panel
6. Exit valve



Fig. 3: Venturimeter

## **EXPT - 3**

### **CHARACTERISTICS OF A CENTRIFUGAL PUMP**

#### **OBJECTIVE :**

1. To determine the characteristics of a Centrifugal Pump at different speed.
2. To construct the characteristic curve in non-dimensional form.

#### **INSTRUCTION :**

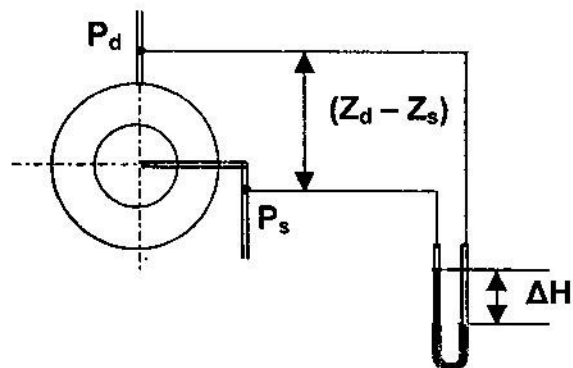
1. Study the setup and make a line diagram.
2. Prime and start the pump.
3. Select a suitable rpm  $N_1$ .
4. Keeping  $N_1$  constant vary the discharge from 0 to the maximum value at finite no. of steps controlling the discharge valve.
5. For each value setting measure the flow rate, the pressure drop across the pump and the input power.
6. Repeat 3 to 5 for  $N_2$  and  $N_3$ .
7. Calculate the head, power and efficiency for all the readings.
8. Construct the characteristic curves for  $N_1$ ,  $N_2$  and  $N_3$ .
9. Plot the  $H - Q$  curve in non-dimensional form using all the data of  $N_1$ ,  $N_2$  and  $N_3$ .
10. Plot the theoretical  $H-Q$  curve for  $N_2$  speed from the experimental data of  $N_1$  speed.

impeller diameter = 99 mm

## PERFORMANCE CHARACTERISTICS OF A CENTRIFUGAL PUMP

**RPM:**

SL NO	Q <sub>DISP</sub>	Q <sub>ACTUAL</sub> (Q <sub>DISP</sub> X η) (m <sup>3</sup> /s)	POWER (kw)	HEAD			HEAD (m) (Computed)	η (%)
				I (cm)	F(cm)	ΔH(cm)		
1								
2								
3								
4								
5								
6								
7								
8								
9								
10								
11								
12								



$$\frac{P_s}{\gamma} + \frac{V_s^2}{2g} + Z_s + H_{pump} = \frac{P_d}{\gamma} + \frac{V_d^2}{2g} + Z_d$$

$$H_{pump}(m) = \frac{P_d - P_s}{\gamma} = \left( \frac{\rho_m - \rho_w}{\rho_w} \right) \Delta H = 0.126 \Delta H \text{ (in cm)}$$



Figure 1: Control Panel

1. Shows input power.
2. Shows rpm and flow rate.
3. Regulator.



Figure 2: Main Setup Back View

1. Centrifugal Pump.
2. Electric Motor.
3. Speedometer.

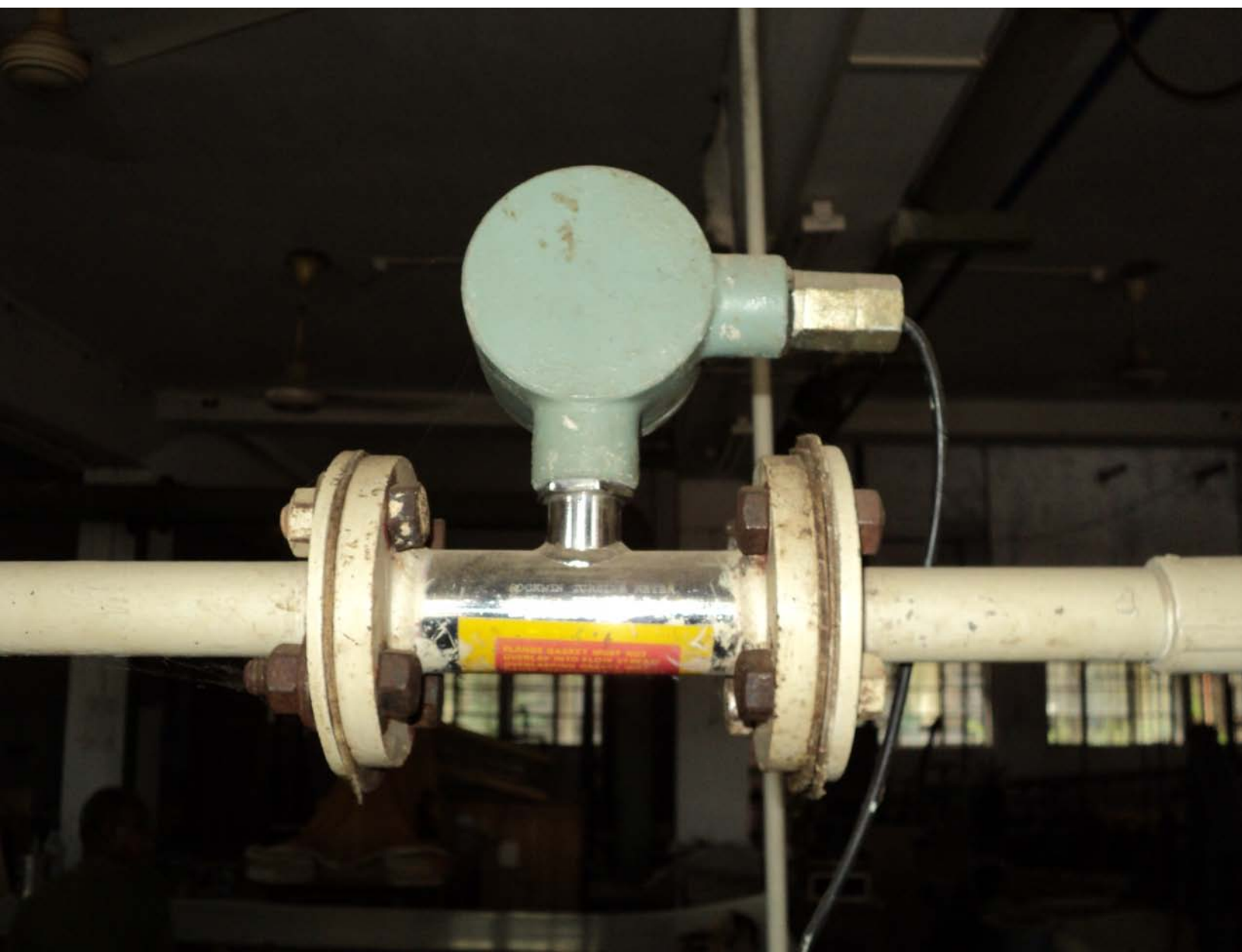


Figure 3: Turbine Meter



Figure 4: Main Setup

## **EXPERIMENT NO. 5**

### **STUDY AND CALIBRATION OF FLOW METERS**

#### **USEFUL DATA:**

#### **ORIFICE METER:**

Orifice diameter: 18.6 mm

Inlet diameter: 26 mm

#### **VENTURI METER:**

Throat diameter: 16 mm

Inlet diameter: 26. 5 mm

**TAKE PIPE LINE DIAMETER = 26 mm  
KINEMATIC VISCOSITY OF WATER =  $10^{-6} \text{ m}^2/\text{s}$**

**CROSS SECTION AREA OF MEASURING TANK = 759mm' X 455mm**

#### **RESULTS TO BE PRESENTED:**

1. Plot of C and  $N_R$  for Orifice meter and Venturi meter [refer to equation (1.3)].
2. Plot  $Q_{\text{actual}}$ ,  $Q_{\text{displayed}}$  and  $N_R$  for all other meters.

## 1.CONSTANT- AREA, VARIABLE- PRESSURE- DROP METERS ("OBSTRUCTION" METERS)

Perhaps the most widely used flowmetering principle involves placing a fixed-area flow restriction of some type in the pipe or duct carrying the fluid. This flow restriction causes a pressure drop which varies with the flow rate; thus measurement of the pressure drop by means of a suitable differential-pressure pickup allows flow-rate measurement. In this section we briefly discuss the most common practical devices that utilize this principle: **the orifice, the flow nozzle, the venturi tube and the Dall flow tube.**

The **sharp-edge orifice** is undoubtedly the most widely employed flowmetering element, mainly because of its simplicity, its low cost, and the great volume of research data available for predicting its behavior. A typical flowmetering setup is shown in Fig.1.1. If one-dimensional flow of an incompressible frictionless fluid without work, heat transfer, or elevation change is assumed, theory gives the volume flow rate  $Q$ , ( $\text{m}^3/\text{s}$ ) as

$$Q = \frac{A_{2f}}{\sqrt{1 - (A_{2f}/A_{1f})^2}} \sqrt{\frac{2(p_1 - p_2)}{\rho}} \quad \dots \dots \dots \quad (1.1)$$

where,  $A_{1f}, A_{2f}$  = cross-section flow areas where  $p_1$  and  $p_2$  are measured,  $\text{m}^2$

$\rho$  = fluid mass density,  $\text{kg/m}^3$

$p_1, p_2$  = static pressure, Pa

We see that measurement of  $Q$  requires knowledge of  $A_{1f}$ ,  $A_{2f}$  and  $\rho$  and measurement of the pressure differential  $p_1 - p_2$ . Actually, the real situation deviates from the assumptions of the theoretical model sufficiently to require experimental correction factors if acceptable flowmetering accuracy is to be attained. For example,  $A_{1f}$  and  $A_{2f}$  are areas of the actual flow cross section, which is not, in general, the same as those corresponding to the pipe and orifice diameters, which are the ones susceptible to practical measurement. Furthermore,  $A_{1f}$  and  $A_{2f}$  may change with flow rate because of flow geometry changes. Also, there are frictional losses that affect the measured pressure drop and lead to a permanent pressure loss. To take these factors into account, an experimental calibration to determine the actual flow rate,  $Q_a$ , is necessary. An expression for  $Q_a$  may be defined as,

$$Q_a = \frac{C_d A_o}{\sqrt{1 - C_c^2 (A_o/A_r)^2}} \sqrt{\frac{2\Delta P}{\rho}} \quad \dots \dots \dots \quad (1.2)$$

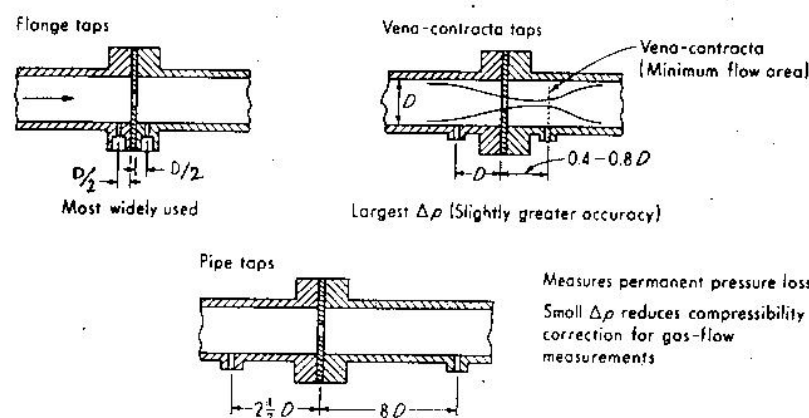
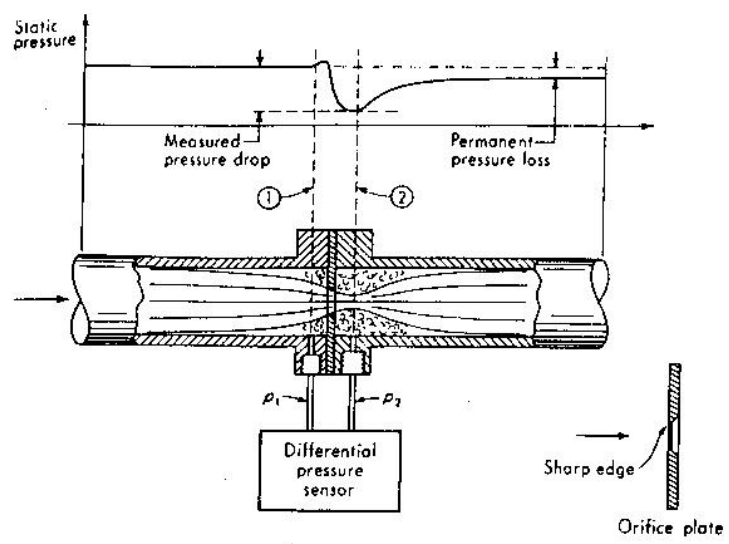


Figure 1.1 Orifice flowmetering.

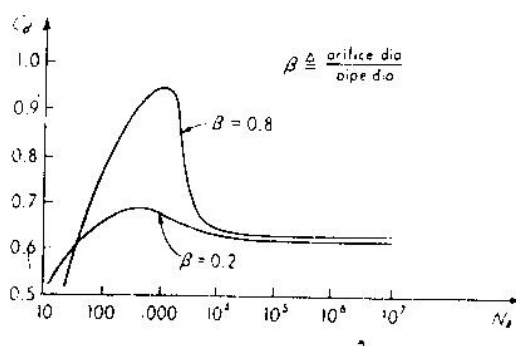


Figure 1.2 Variation in discharge coefficient.

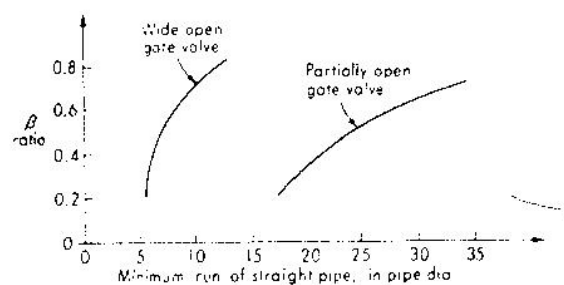


Figure 1.3 Effect of upstream disturbances.

where,  $A_p$  = pipe cross-section area,  $A_o$  = orifice cross-section area,  $C_c$  and  $C_d$  are the coefficient of contraction and discharge respectively and  $\Delta P$  is the measured differential pressure. However, a simplified formula is generally used to obtain  $Q_a$  and is given as,

$$Q_a = C \cdot A_o \sqrt{\frac{2\Delta P}{\rho}} \quad \text{for a given } \beta = D_o/D_p \quad \dots \dots \dots \quad (1.3)$$

where, **C** = flow coefficient,  $D_o$  = Orifice or Venturi throat diameter,  $D_p$  = Pipeline diameter.

The discharge coefficient of a given installation varies mainly with the Reynolds number  $N_R$  at the orifice. Thus the calibration can be performed with a single fluid, such as water, and the results used for any other fluid as long as the Reynolds numbers are the same. Variation of  $C_d$  with  $N_R$  follows typically the trend of Fig.1.2. While the above discussion would seem to indicate that each installation must be individually calibrated, fortunately this is not the case. If one is willing to construct the orifice according to certain standard dimensions and to locate the pressure taps at specific points, then quite accurate (about 0.4 to 0.8 percent error) values of  $C_d$  may be obtained based on many past experiments. It also should be noted that the standard calibration data assume no significant flow disturbances such as elbows, bends, tees, valves, etc., for certain minimum distance upstream of the orifice. The presence of such disturbances close to the orifice can invalidate the standard data, causing errors of as much as 15 percent. Information on the minimum distances is available. Fig. 1.3 shows a typical example. If the minimum distances are not feasible, straightening vanes may be introduced ahead of the flowmeter to smooth out the flow.

Since flow rate is proportional to  $\sqrt{\Delta p}$  a 10:1 change in  $\Delta p$  corresponds to only about a 3:1 change in flow rate. Since a given  $\Delta p$ -measuring instrument becomes quite inaccurate below about 10 percent of its full-scale reading, this non-linearity typical of all obstruction meters restricts the accurate range of flow measurement to about 3:1. That is, a meter of this type cannot be used accurately below about 30 percent of its maximum flow rating.

The orifice has the largest permanent pressure loss of any of the obstruction meters. This is one of its disadvantages since it represents a power loss that must be replaced by whatever pumping machinery is causing the flow. The permanent pressure loss is given approximately by  $\Delta p(1 - \beta^2)$ , where  $\Delta p$  is the differential pressure used for flow measurement. Thus for the usual range of  $\beta$  (0.2 to 0.7), the permanent pressure loss ranges from 0.96  $\Delta p$  to 0.51  $\Delta p$ . The actual power loss, in fact, may be quite small since the  $\Delta p$

recommended for conventional flowmetering of liquids is only 20 to 400 in of water (0.72 to 14.4 lb/in<sup>2</sup>).

Orifice discharge coefficients are quite sensitive to the condition of the up-stream edge of the hole. The standard orifice design requires that this edge be very sharp and that the orifice plate be sufficiently thin relative to its diameter. Wear (rounding) of this sharp edge by long use or abrasive particles can cause significant changes in the discharge coefficient. Flows that contain suspended solids also cause difficulty since the solids tend to collect behind the "dam" formed by the orifice plate and cause irregular flow. Often this problem can be solved by use of an "eccentric" orifice in which the hole is at the bottom of the pipe rather than on the centerline. This allows the solids to be swept through continuously. Liquids containing traces of vapor or gas may be metered if the orifice is installed in a vertical run of pipe with the flow upward. Gases containing traces of liquid may be similarly handled except that the flow should be downward.

When compressible fluids are metered, by assuming an isentropic process between states 1 and 2, the following relation may be derived for compressible fluids:

$$W = C_d A_2 \sqrt{\frac{2gkp_1}{(k-1)v_1}} \sqrt{\frac{(p_2/p_1)^{2/k} - (p_2/p_1)^{(k+1)/k}}{1 - \beta^4 (p_2/p_1)^{2/k}}} \quad \dots \quad (1.4)$$

where, W = weight flow rate, 1bf/s

k = ratio of specific heats (1.4 for air)

g = local gravity

v<sub>1</sub> = specific volume at state 1, ft<sup>3</sup>/1bf

The discharge coefficient C<sub>d</sub> is the same for liquids or gases as long as the Reynolds number is the same. In many practical gas-flow installations, the meter pressure drop is so small that the pressure ratio P<sub>2</sub>/P<sub>1</sub> is 0.99 or greater. Under these conditions, the simpler incompressible relation of Eq. (1.2) may be used with an error less than 0.6 percent if, for example, β = 0.5 and k = 1.4. Modified to give weight rather than volume flow rate, this is

$$W = C_d A_2 \left[ \sqrt{1 - \left( \frac{A_2}{A_1} \right)^2} \right]^{-1} \sqrt{\frac{2g(p_1 - p_2)}{v_1}} \quad \dots \quad (1.5)$$

For P<sub>2</sub>/P<sub>1</sub> < 0.99, the error becomes greater, being 6 percent at P<sub>2</sub>/P<sub>1</sub> = 0.9, 12 percent at 0.8, 19 percent at 0.7, and 26 percent at 0.6 (if β = 0.5 and k = 1.4). For such situations, the more complex compressible formula obviously must be used. In flow nozzles and venturis, the

flow process is close enough to isentropic to allow theoretical calculation of compressibility effects from Eq. (1.4). In orifices, however, deviation from isentropic conditions is significant (greater turbulence), and an experimental compressibility factor  $Y$  is used in the equation:

$$W = Y \left\{ C_d A_2 \left[ \sqrt{1 - \left( \frac{A_2}{A_1} \right)^2} \right]^{-1} \right\} \sqrt{\frac{2g(p_1 - p_2)}{v_1}} \quad \dots \dots \dots \quad (1.6)$$

For flange taps or vena-contracta taps

$$Y = 1 - (0.41 + 0.35\beta^4) \frac{p_1 - p_2}{p_1} \frac{1}{k} \quad \dots \dots \dots \quad (1.7)$$

while for pipe taps

$$Y = 1 - [0.333 + 1.145(\beta^2 + 0.7\beta^5 + 12\beta^{13})] \frac{p_1 - p_2}{p_1} \frac{1}{k} \quad \dots \dots \dots \quad (1.8)$$

These empirical formulas are accurate to  $\pm 0.5$  percent if  $0.8 < p_2 / p_1 < 1.0$  and the flowing fluid is a gas or vapor other than steam. For steam the accuracy is  $\pm 1.0$  percent. In sizing orifices for gas measurement, a useful rule of thumb is that the maximum  $\Delta p$  (in inches of water) should not exceed the upstream gage pressure in pounds per square inch. Handbooks published by flowmeter manufacturers provide many practical guidelines and timesaving charts for orifice selection and application.

The **flow nozzle, venturi tube, and Dall flow tube** (Fig. 1.4) all operate on exactly the same principle as the orifice; the significant differences lie in the numerical values of certain characteristics. Discharge coefficients of flow nozzles and venturis are larger than those for orifices and also exhibit an opposite trend with Reynolds numbers, varying from about 0.94 at  $N_R = 10,000$  to 0.99 at  $N_R = 106$ . The Dall-flow-tube coefficient is more like that of an orifice; for  $\beta = 0.7$ , for example, it goes from about 0.68 at  $N_R = 100,000$  to 0.66 at  $N_R = 10^6$ . Individual calibrations generally are needed on all these devices since their complicated shapes (compared with an orifice) make accurate reproduction difficult.

When comparing the permanent pressure losses of the various devices, you should require that each device be producing the same measured  $\Delta p$ , since this would keep the accuracy constant. On this basis, the permanent pressure loss of a flow nozzle is practically identical with that of an orifice, because, to get the same  $\Delta p$ , the flow nozzle must have a smaller  $\beta$

ratio, and losses increase with decreasing  $\beta$  ratio. The venturi tube also requires a smaller  $\beta$  for a given  $\Delta p$ , but because of its streamlined form, its losses are low and nearly independent of  $\beta$ . The permanent pressure loss is of the order of 10 to 15 percent of the measured  $\Delta p$  over the range  $0.2 < \beta < 0.8$ ; thus a venturi gives a definite improvement in power losses over an orifice and often is indicated for measuring very large flow rates, where power losses, though a small percentage, become economically significant in absolute value. The initial higher cost of a venturi over an orifice thus may be offset by reduced operating costs. The Dall flow tube has the unexpected (though desirable) features of a high measured  $\Delta p$  (similar to an orifice) and a low permanent pressure loss (similar to, and sometimes better than, a venturi). These apparently inconsistent virtues have been checked experimentally, but are not fully explained theoretically. The permanent pressure loss of a Dall tube is of the order of 50 percent or less of that of a venturi tube with the same  $\Delta p$ . Other factors to consider in choosing among the orifice, flow nozzle, venturi, and Dall tube include freedom from pressure-tap clogging resulting from suspended solids (venturi is best), loss of accuracy due to wear (venturi, flow nozzle, and Dall tube are better than an orifice), accuracy (venturi, when calibrated, is best), cost, and ease of changing the flow element to a different size.

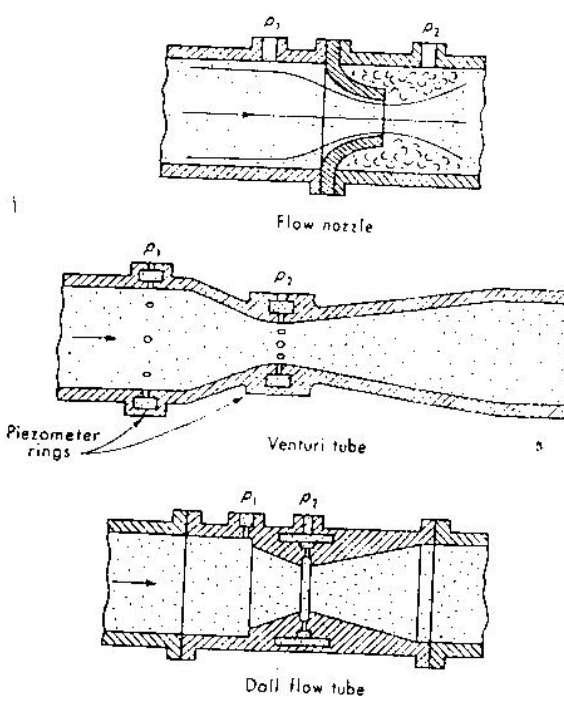


Figure 1.4 Variable-pressure drop flowmeters.

## 2. CONSTANT-PRESSURE-DROP, VARIABLE-AREA METERS (ROTAMETERS)

A rotameter consists of a vertical tube with tapered bore in which a "float" assumes a vertical position corresponding to each flow rate through the tube (see Fig.2.1). For a given flow rate, the float remains stationary since the vertical forces of differential pressure, gravity, viscosity, and buoyancy are balanced. This balance is self-maintaining since the meter flow area (annular area between the float and tube) varies continuously with vertical displacement; thus the device may be thought of as an orifice of adjustable area. The downward force (gravity minus buoyancy) is constant, and so the upward force (mainly the pressure drop times the float cross-section area) must be constant also. Since the float area is constant, the pressure drop must be constant. For a fixed flow area,  $\Delta p$  varies with the square of flow rate, and so to keep  $\Delta p$  constant for differing flow rates, the area must vary. The tapered tube provides this variable area. The float position is the output of the meter and can be made essentially linear with flow rate by making the tube area vary linearly with the vertical distance. Rotameters thus have an accurate range of about 10 : 1, considerably better than square root-type elements. Accuracy is typically  $\pm 2$  percent full scale ( $\pm 1$  percent if calibrated) with repeatability about 0.25 percent of reading. Assuming incompressible flow and the above described simplified model, we can derive the result

$$Q = \frac{C_d (A_t - A_f)}{\sqrt{1 - [(A_t - A_f)/A_t]^2}} \sqrt{2gV_f \frac{w_f - w_{ff}}{A_f w_{ff}}} \quad \dots \dots \dots \quad (2.1)$$

where,  $Q$  = volume flow rate,  $\text{m}^3/\text{s}$ ,  $C_d$  = discharge coefficient

$A_t$  = area of tube,  $\text{m}^2$ ,  $A_f$  = area of float,  $\text{m}^2$ ,  $g$  = local gravity,  $\text{m}/\text{s}^2$

$V_f$  = volume of float,  $\text{m}^3$ ,  $w_f$  = specific weight of float,  $\text{kg}/\text{m}^3$

$w_{ff}$  = specific weight of flowing fluid,  $\text{kg}/\text{m}^3$

If the variation of  $C_d$  with float position is slight and if  $[(A_t - A_f)/A_t]^2$  is always much less than 1, then Eq. (2.1) has the form

$$Q = K (A_t - A_f) \quad \dots \dots \dots \quad (2.2)$$

And if the tube is shaped so that  $A_t$  varies linearly with float position  $x$ , then  $Q = K_1 + K_2 x$ , a linear relation. The floats of rotameters may be made of various materials to obtain the

desired density difference [ $w_f - w_{ff}$  in Eq. (2.1)] for metering a particular liquid or gas. Some float shapes, such as spheres, require no guiding in the tube; others are kept central by guide wires or by internal ribs in the tube. Floats shaped to induce turbulence can give viscosity insensitivity over a 100 : 1 range. The tubes often are made of high-strength glass to allow direct observation of the float position. Where greater strength is required, metal tubes can be used and the float position detected magnetically through the metal wall. If a pneumatic or an electrical signal related to the flow rate is desired, the float motion can be measured with a suitable displacement transducer. Flow rates beyond the range of the largest rotameter may be measured by combining an orifice plate and a rotameter in a bypass arrangement.

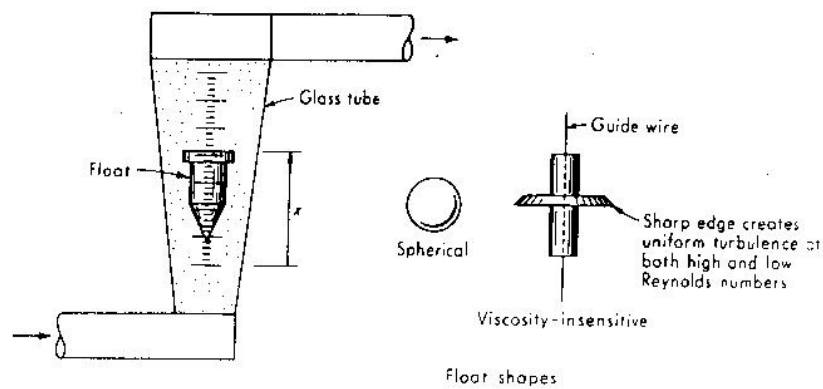


Figure 2.1 Rotameter.

### 3. TURBINE METERS

If a turbine wheel is placed in a pipe containing a flowing fluid, its rotary speed depends on the flow rate of the fluid. By reducing bearing friction and keeping other losses to a minimum, one can design a turbine whose speed varies linearly with flow rate; thus a speed measurement allows a flow-rate measurement. The speed can be measured simply and with great accuracy by counting the rate at which turbine blades pass a given point, using a magnetic proximity pickup to produce voltage pulses. By feeding these pulses to an electronic pulse-rate meter, one can measure flow rate; by accumulating the total number of pulses during a timed interval, the total flow is obtained. These measurements can be made very accurately because of their digital nature. If an analog voltage signal is desired, the pulses can be fed to a frequency-to-voltage converter. Fig.3.1 shows a flowmetering system of this type.

Dimensional analysis of the turbine flowmeter shows that (if bearing friction and shaft power output are neglected) the following relation should hold :

$$\frac{Q}{n D^3} = \text{some function of } \frac{n D^2}{\gamma} \quad \dots \dots \dots \quad (3.1)$$

where,  $Q$  = volume flow rate,  $\text{m}^3/\text{s}$

$n$  = rotor angle velocity,  $\text{r/s}$

$D$  = meter bore diameter,  $\text{m}$

$\gamma$  = kinematic viscosity,  $\text{m}^2/\text{s}$

Actually, the effect of viscosity is limited mainly to low flow rates, with high flow rates being in the turbulent regime where viscosity effects are secondary. For negligible viscosity effects, a simplified analysis based on strictly kinematic relationships gives the following result:

$$\frac{Q}{n D^3} = \frac{\pi L}{4 D} \left[ 1 - \alpha^2 - \frac{2 m (D_b - D_h)}{\pi D^2} t \sqrt{1 + \left( \frac{\pi D_b}{L} \right)^2} \right] \quad \dots \dots \dots \quad (3.2)$$

where,  $L$  = rotor lead,  $\text{m}$

$\alpha = D_h / D$

$m$  = number of blades

$D_b$  = rotor-blade-tip diameter,  $\text{m}$

$D_h$  = rotor-hub diameter,  $\text{m}$

$t$  = rotor-blade thickness,  $\text{m}$

Equation (3.2) gives  $Q = Kn$ , where  $K$  is a constant for any given meter and is independent of fluid properties. Thus this represents the ideal situation. Deviations from this ideal may be found from experimental calibrations, such as are shown for a meter with  $D = 25$  mm in Fig.3.2. We see for sufficiently high values of  $nD^2/\gamma$  that  $Q/(nD^3)$  becomes essentially constant, as predicted by Eq. (3.2). In the particular case shown,  $Q/(nD^3) = 1.92$  for at least a 10 : 1 range of  $nD^2/\gamma$ ; thus this would be a useful linear operating range for this meter. The meter could be utilized at lower flow rates by applying corrections obtained from Fig.3.2. However, usually this is not done since turbine meters are available in a wide range of sizes, each being linear over a different flow range. If the total flow range to be accommodated is about 10 : 1 or less, one can usually select a turbine meter that is linear in the desired range. Linearity is particularly desirable if one is totalizing pulses to get a total flow over a timed interval during which flow rate fluctuates.

At low flow rates, linearity is degraded by both viscous effects and magnetic pickup drag. The latter can be reduced by using a modulated carrier type of pickoff. These are recommended for all gas applications in meters of size 1 in or less and for any liquid applications where extended linear ranges are necessary.

Commercial turbine meters are available with full-scale flow rates ranging from about 0.01 to 30,000 gal/min for liquids and 0.01 to 15,000 ft<sup>3</sup>/min for air. Nonlinearity within the design range (usually about 10 : 1) can be as good as 0.05 percent in the larger sizes. The output voltage of the magnetic pickups is of the order of 10 mV rms at the low end of the flow range and 100 mV at the high. Pressure drop across the meter varies with the square of flow rate and is about 3 to 10 lb/in<sup>2</sup> at full flow.

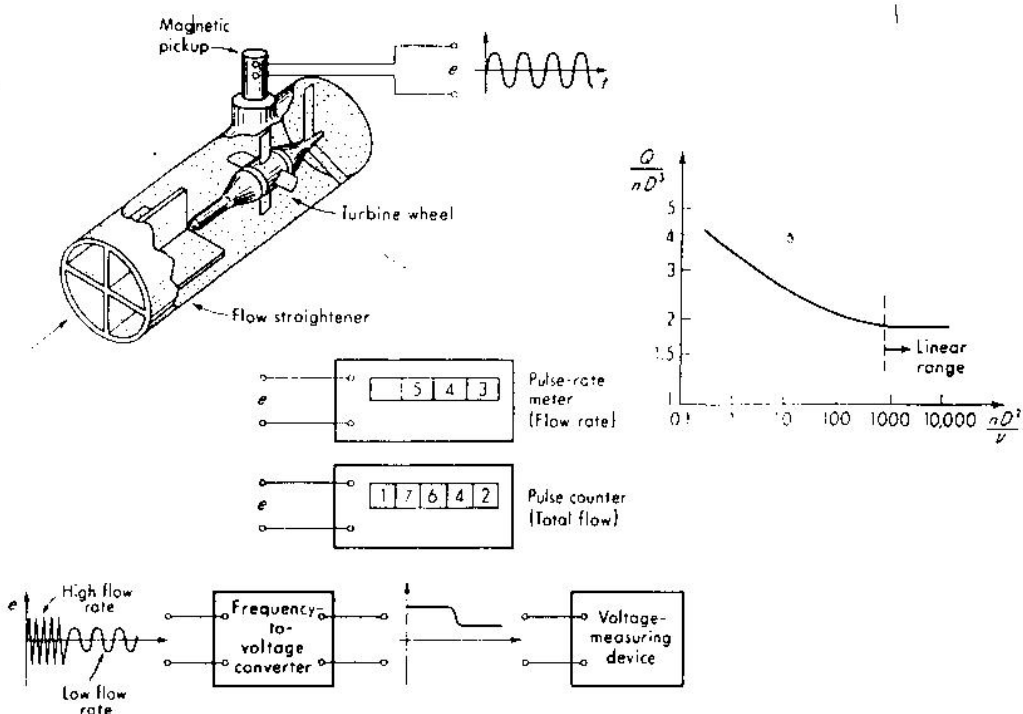


Figure 3.1 Turbine flowmeter.

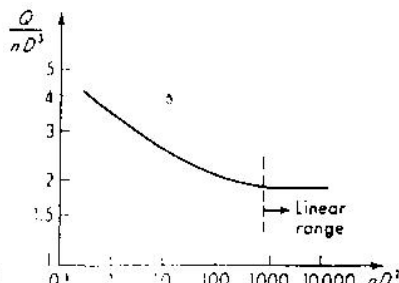


Figure 3.2 Turbine flowmeter characteristics.

## 4. ULTRASONIC FLOWMETER

### Measuring principle

A sound wave traveling in the direction of flow of the fluid requires less time between one fixed point and another than one traveling in the opposite direction. This is the principle employed to measure the flow rate with ultrasonic waves. Different flight times are an indication of the flow velocity of the fluid concerned.

**Double-beam version:** The ultrasonic sensors A + B and A' + B' are located in symmetrical arrangement on the outside of the measuring tube.

**Single-beam version:** The ultrasonic sensors A + B are located in symmetrical arrangement on the outside of the measuring tube at an angle of 180°.

Each line of measurement (A + B and A' + B') forms an angle  $\varphi$  with the tube centerline.

The ultrasonic waves travel from point A to point B at speed

$$V_{AB} = c_0 + V_m \times \cos \varphi \quad (4.1)$$

and, conversely, from point B to point A at speed

$$V_{BA} = c_0 - V_m \times \cos \varphi \quad (4.2)$$

The following applies to the different flight times from points A to B,

$$t_{AB} = \frac{L}{c_0 + V_m \times \cos \varphi} \quad (4.3)$$

and from point B to A,

$$t_{BA} = \frac{L}{c_0 - V_m \times \cos \varphi} \quad (4.4)$$

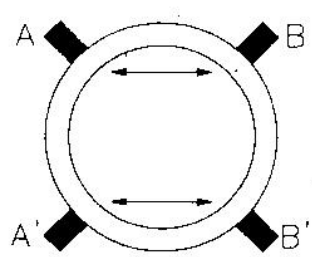
The mean flow velocity  $V_m$  of the product is calculated using the last two equations:

$$v_m = GK \frac{t_{BA} - t_{AB}}{t_{BA} \times t_{AB}} \quad (4.5)$$

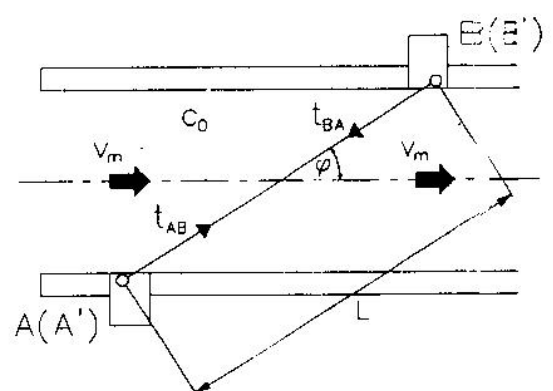
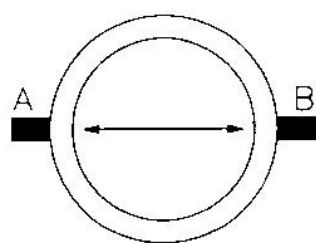
$t_{AB}$  and  $t_{BA}$  are measured continuously.

A (A')	Transmitter and receiver
B (B')	Transmitter and receiver
L	Distance between ultrasonic sensors
$v_m$	Average flow velocity of fluid
$t_{AB}$ ( $v_{AB}$ )	Time of flight (propagation speed) of sound waves from points B to A
$c_0$	Sound velocity in the medium (fluid)
GK	Calibration constant
$\varphi$	Angle between tube centerline and line of measurement

Double-beam



Single-beam



## 5. ELECTROMAGNETIC FLOWMETERS

The electromagnetic flowmeter is an application of the principle of induction, shown in Fig.5.1. If a conductor of length  $l$  moves with a transverse velocity  $v$  across a magnetic field of intensity  $B$ , there will be forces on the charged particles of the conductor that will move the positive charges toward one end of the conductor and the negative charges to the other. Thus a potential gradient is set up along the conductor, and there is a voltage difference  $e$  between its two ends. The quantitative relation among the variables is given by the well-known equation

$$e = Blv \quad \dots \dots \dots \quad (5.1)$$

where,  $B$  = field flux density,  $\text{Wb/m}^2 = \text{V} \cdot \text{s/m}^2$

$l$  = conductor length, m

$v$  = conductor velocity, m/s

If the ends of the conductor are connected to some external circuit that is stationary with respect to the magnetic field, the induced voltage, in general, will cause a current  $i$  to flow. This current flows through the moving conductor, which has a resistance  $R$ , causing an  $iR$  drop, so that the terminal voltage of the moving conductor becomes  $e - iR$ .

We consider now a cylindrical jet of conductive fluid with a uniform velocity profile, traversing a magnetic field as in Fig.5.1b. In a liquid conductor the positive and negative ions are forced to opposite sides of the jet, giving a potential distribution as shown. The maximum voltage difference is found across the ends of a horizontal diameter and is  $BD_p v$  in magnitude. In a practical situation, the magnetic field is of limited extent, as in Fig.5.1c; thus no voltage is induced in that part of the jet outside the field. Since these parts of the fluid are, however, still conductive paths, they tend partially to "short-circuit" the voltages induced in the section exposed to the field; thus the voltage is reduced from the value  $BD_p v$ . If the field is sufficiently long, this effect will be slight at the center of the field length. A length of 3 diameters usually is sufficient.

In a practical flowmeter (see Fig.5.2), the "jet" is contained within a stationary pipe. The pipe must be nonmagnetic to allow the field to penetrate the fluid and usually is nonconductive (plastic, for instance), so that it does not provide a short-circuit path between the positive and negative induced potentials at the fluid surface. This nonconductive pipe has two electrodes placed at the points of maximum potential difference. These electrodes then

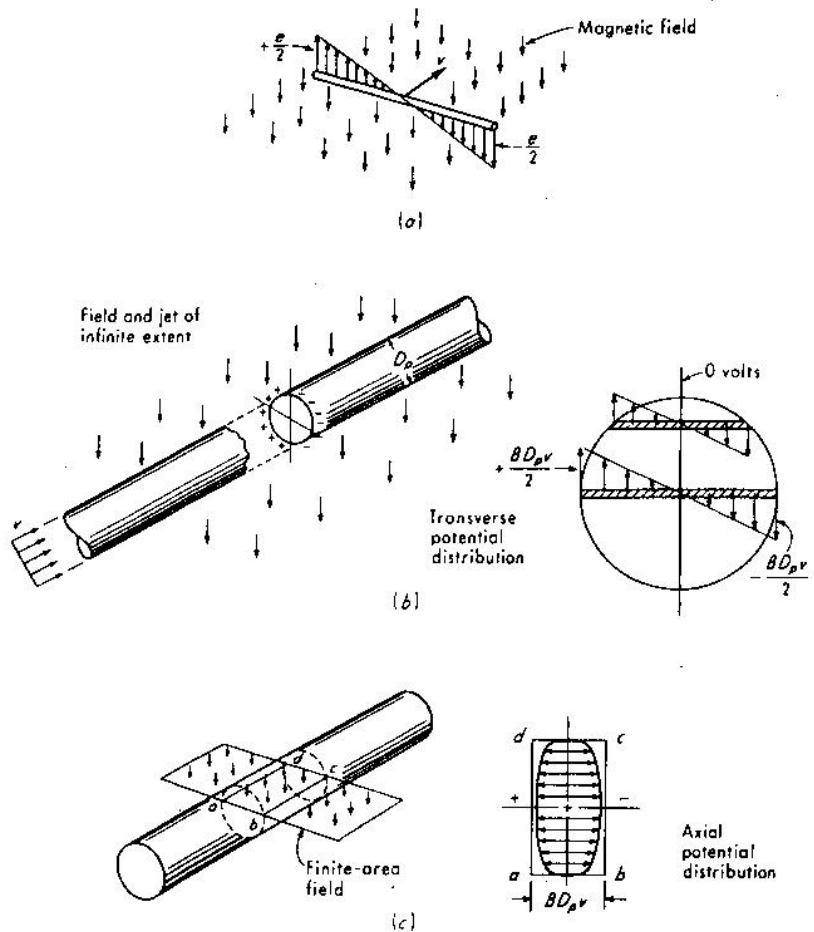


Figure 5.1 Electromagnetic flowmeter.

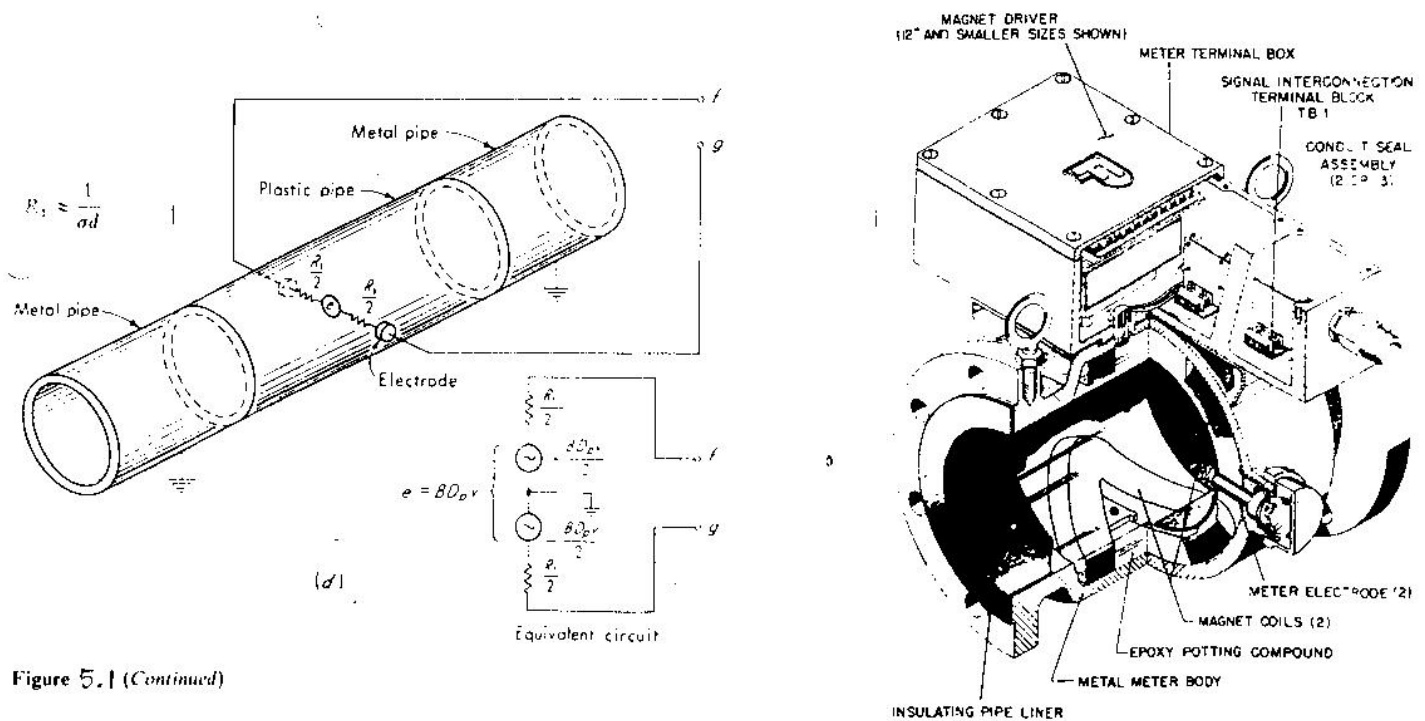


Figure 5.1 (Continued)

Figure 5.2 Construction details of magnetic flowmeter

supply a signal voltage to external indicating or recording apparatus. While Fig.5.1 shows a uniform velocity profile, it has been proved mathematically that  $e$  corresponds to the average velocity of any profile which is symmetric about the pipe centerline. Because it is impractical to make the entire piping installation nonconductive, a short length (the flowmeter itself) of nonconductive pipe must be coupled into an ordinary metal-pipe installation. Since the fluid itself is conductive, this means that there is a conductive path between the electrodes. In Fig.5.1d, this path is shown split into two equal parts  $R_t/2$  and containing the signal source  $e = BD_p v$ . This resistance is not simple to calculate since it involves a continuous distribution of resistance over complex bodies. However, it can be estimated from theory, and once a device is built, it can be directly measured. The magnitude of this source resistance determines the loading effect of any external circuit connected to the electrodes.

The magnetic field used in such a flowmeter conceivably could be either constant or alternating, giving rise to a dc or an ac output signal, respectively. For many years, ac systems (50 or 60 Hz) were most common, since they reduced polarization effects at the electrodes, did not cause flow-profile distortion from magnetohydrodynamic-effects, could use high-pass filtering to eliminate slow, spurious voltage drifts resulting from thermocouple and galvanic actions, and allowed use of high-gain ac amplifiers whose drift was less than that of dc types of comparable gain. These advantages outweighed the major disadvantage that the powerful ac field coils induced spurious ac signals into the measurement circuit. To cancel this error, one had to periodically stop the flow to get a pipe-full, zero-velocity condition and then adjust a balance control to get a zero output reading.

About 1975, industrial meters utilizing an "interrupted dc" field became available, and currently the market is shared mainly by these two types. In the interrupted dc meter, a dc field is switched in a square-wave fashion between the working value and zero, at about 3 to 6 Hz. When the field is zero, any instrument output that appears is considered to be an error; thus by storing this zero error and subtracting it from the total instrument output obtained when the field is next applied, one implements an "automatic zero" feature which corrects for zero errors several times a second. Additional advantages include power savings of up to 75 percent and simpler wiring practices. A disadvantage in some applications is the slower response time of about 7 s (60-Hz systems have about 2 s).

For a 60-Hz ac system with tapwater flowing at 100 gal/min in a 3-in- diameter pipe,  $e$  is about 3 mV rms. The resistance between the electrodes is given by theory as approximately  $1/(\sigma d)$ , where  $\sigma$  = fluid conductivity and  $d$  = electrode diameter. For tapwater,

$\sigma \approx 200 \mu\text{S}/\text{cm}$ ; so if  $d \approx 0.64 \text{ cm}$ , there is a resistance of about  $7,800 \Omega$  as the internal resistance of the voltage source producing  $e$ , which requires the sensor amplifier to have an input impedance that is large relative to this value. Standard magnetic flowmeters accept fluids with conductivities as low as about  $5 \mu\text{S}/\text{cm}$ , with special systems going down to about  $0.1 \mu\text{S}/\text{cm}$ . Gasoline, with  $10^{-8} \mu\text{S}/\text{cm}$ , is definitely not measurable; alcohol, with  $0.2 \mu\text{S}/\text{cm}$ , is just barely measurable; mercury (a liquid metal), with  $10^{10} \mu\text{S}/\text{cm}$ , presents no conductivity problem. While commercially available systems are limited to the  $0.1 \mu\text{S}/\text{cm}$  value, research devices which work with dielectric fluids such as liquid hydrogen have been demonstrated.

## 6. VORTEX-SHEDDING FLOWMETERS

The phenomenon of vortex shedding ("Karman vortex street") downstream of an immersed solid body of "blunt" shape when a steady flow impinges upstream is well known in fluid mechanics and is the basis of the vortex-shedding flowmeter. When the pipe Reynolds number  $N_R$  exceeds about 10,000, vortex shedding is reliable, and the shedding frequency  $f$  given by

$$f = \frac{N_{st} V}{d} \quad \dots \dots \dots \quad (6.1)$$

where,  $V$  = fluid velocity

$d$  = characteristic dimension of shedding body

$N_{st}$  = Strouhal number, an experimentally determined number, nearly constant in the useful flowmetering range (for example, 0.21 for cylinders)

By proper design of the shedding body shape,  $N_{st}$  can be kept nearly constant over a wide range of  $N_R$  (and thus flow rate), making  $f$  proportional to  $V$  and thus giving a "digital" flowmetering principle based on counting the vortex shedding rate (see Fig. 6.1). Various shedder shapes and frequency sensing schemes have been developed by several manufacturers. The vortices cause alternating forces or local pressures on the shedder; piezoelectric and strain-gage methods can be employed to detect these. Hot-film thermal anemometer sensors buried in the shedder can detect the periodic flow-velocity fluctuations. The interruption of ultrasonic beams by the passing vortices can be used to count them. Vortex-induced differential pressures will cause oscillation of a small caged ball whose motion can be detected with a magnetic proximity pickup. Fig. 6.2 shows yet another scheme which senses differential pressure with an elastic diaphragm. A wide variety of liquids and gases and steam may be metered. Linear ranges of 15 : 1 are common, with 200 : 1 sometimes possible. Vortex frequencies at maximum flow rate are the order of 200 to 500 Hz, and the frequency responds to changing flow rate within about 1 cycle.

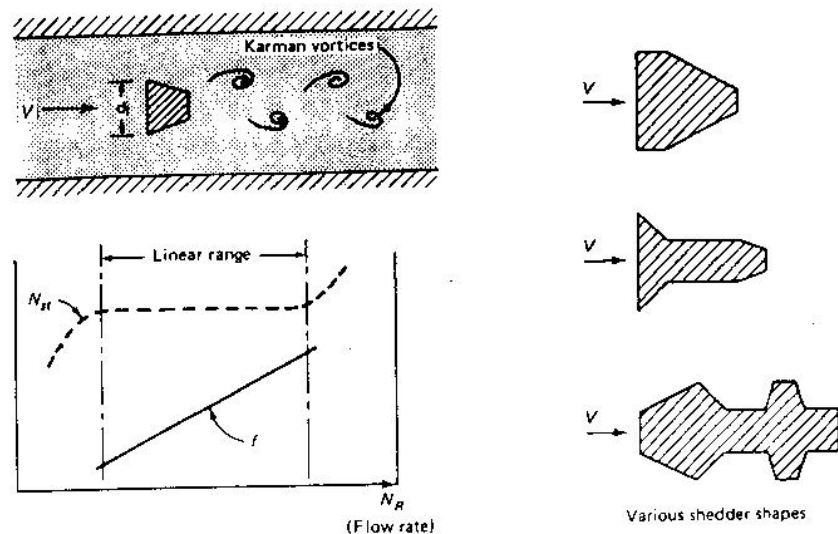


Figure 6.1 Vortex-shedding flowmeter principles.

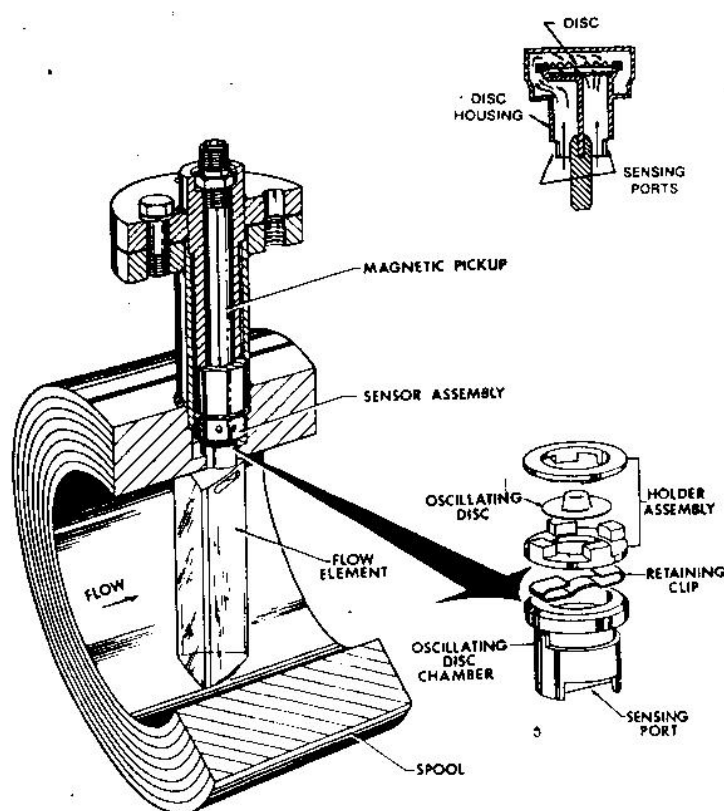


Figure 6.2 Vortex-shedding flowmeter details. (Courtesy Neptune Eastech, Edison, N.J.)

Turbine	Electromagnetic	Vortex-Shedding	Ultrasonic	Actual Flow Rate ( $Q_a$ )	Reynolds Number

Table 1: Flow meters reading in lpm And Reynolds number calculation.

Left Column ( $H_1$ )	Right Column ( $H_2$ )	Column Difference ( $H_d$ )	Pressure Difference (P)	( $C_d$ )	Flow Rate ( $Q_i$ )

Table 2: Venturi meter readings. Where  $C_d$  is coefficient of discharge.

Left Column ( $H_1$ )	Right Column ( $H_2$ )	Column Difference ( $H_d$ )	Pressure Difference (P)	( $C_d$ )	Flow Rate ( $Q_i$ )

Table 3: Orifice meter readings. Where  $C_d$  is coefficient of discharge.

Initial Laval ( $H_1$ )	Final Laval ( $H_2$ )	Difference ( $H_d$ )	Time (t)	Actual Flow Rate ( $Q_a$ )

Table 4: Tank data.



Figure 1: Constant-Area, Variable-Pressure-Drop Meters

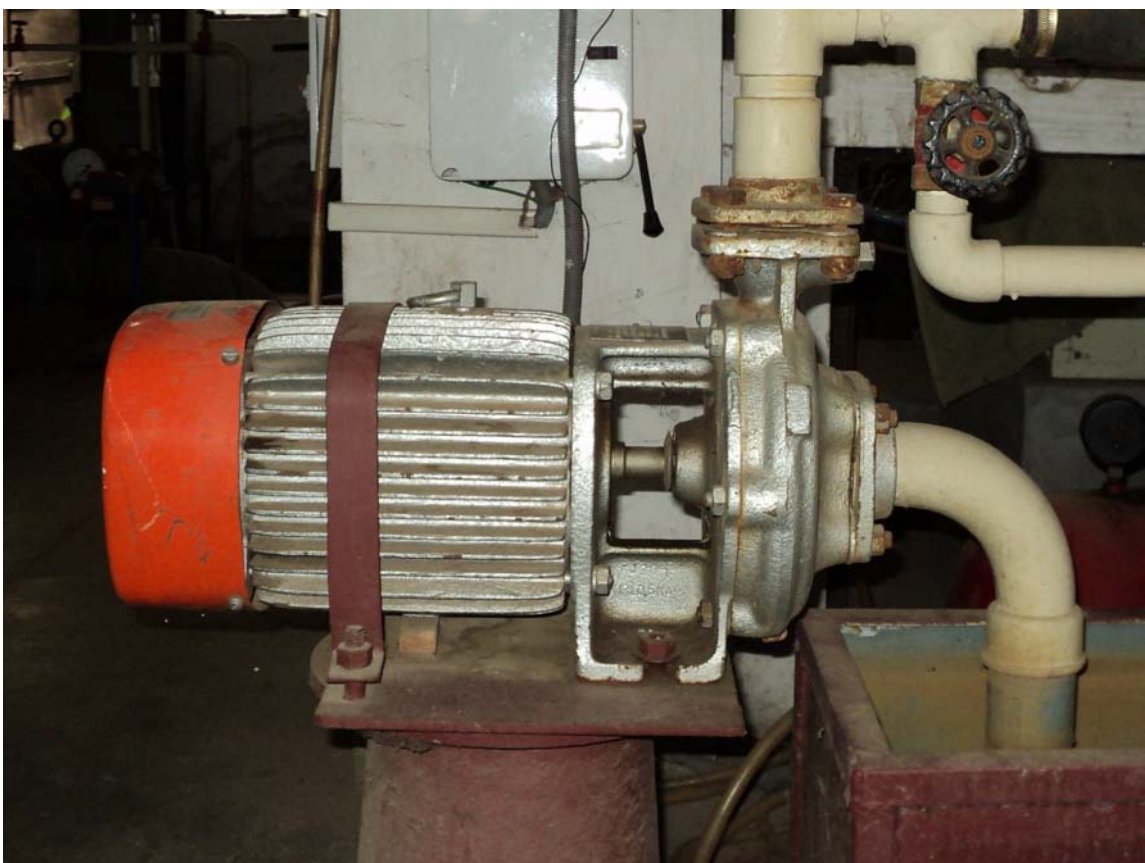


Figure 2: Centrifugal Pump To Supply Water

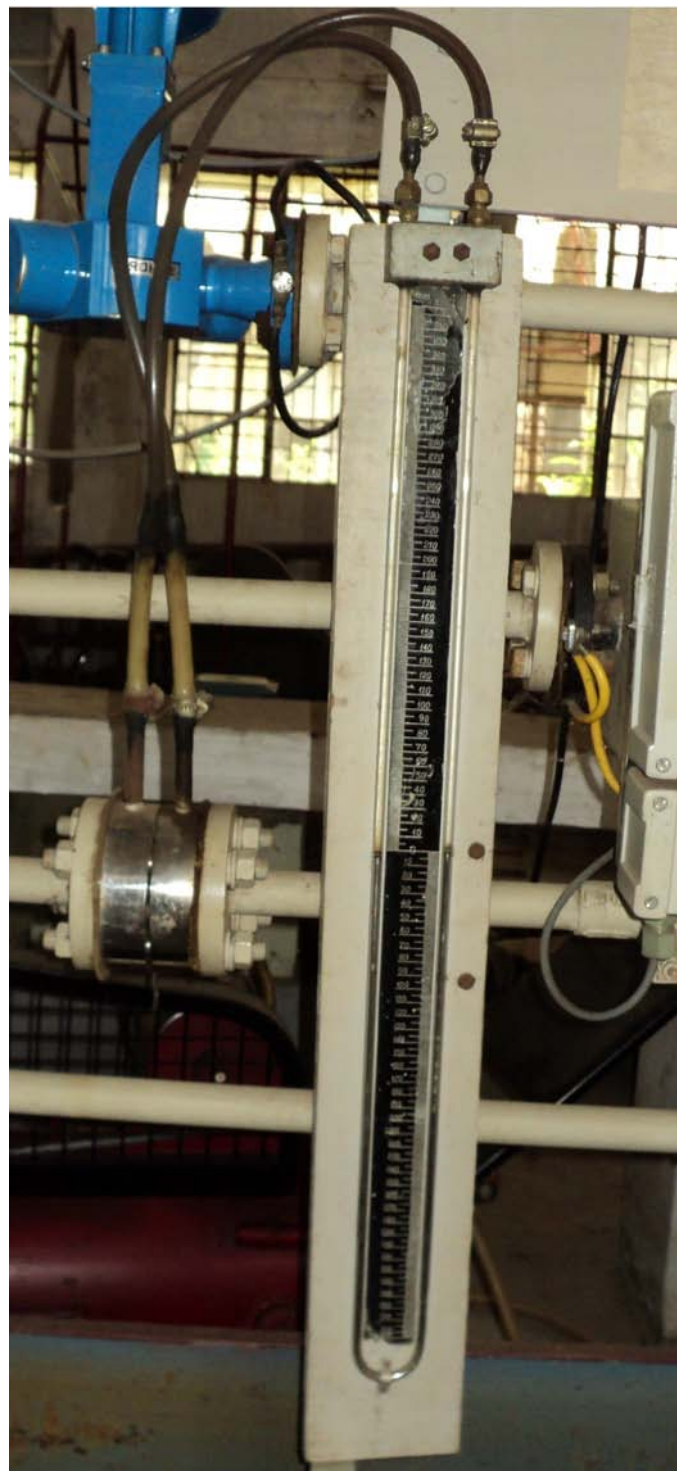


Figure 3: Orifice Meter

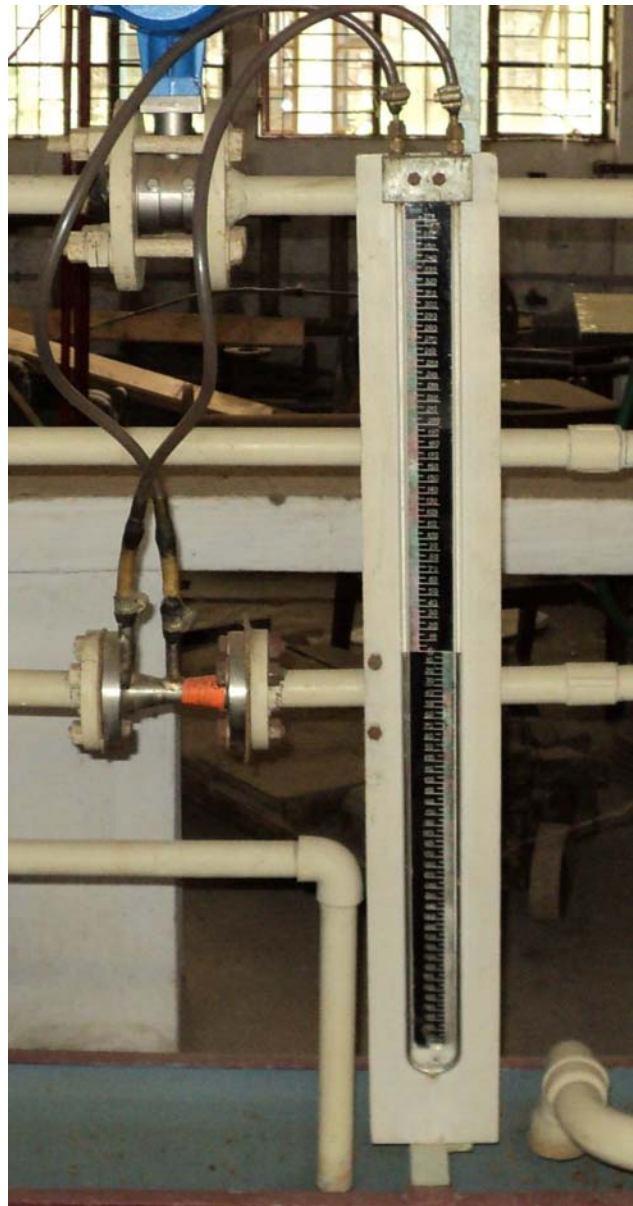


Figure 4: Venturimeter



Figure 5: Rota-meter

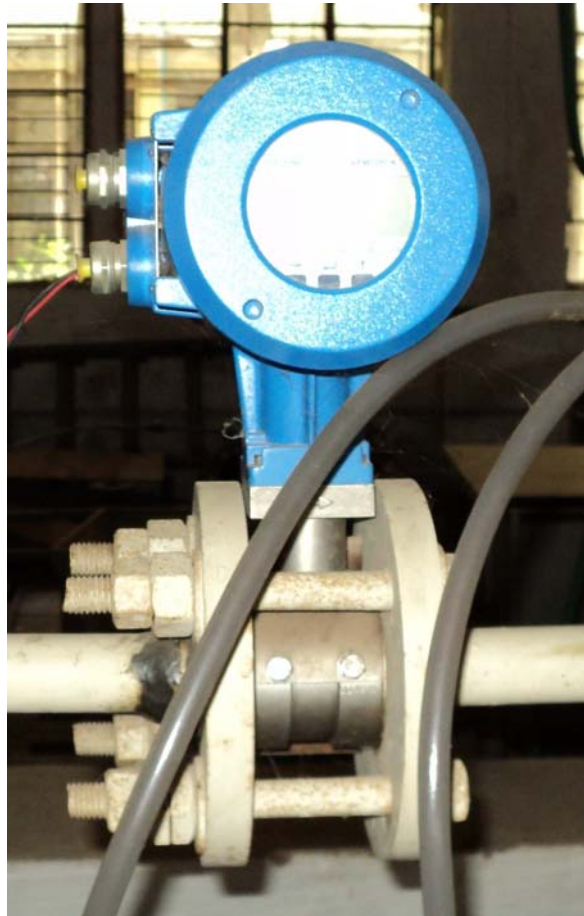


Figure 6: Vortex-Shedding Flow-meter



Figure 7: Ultrasonic Flow-meter

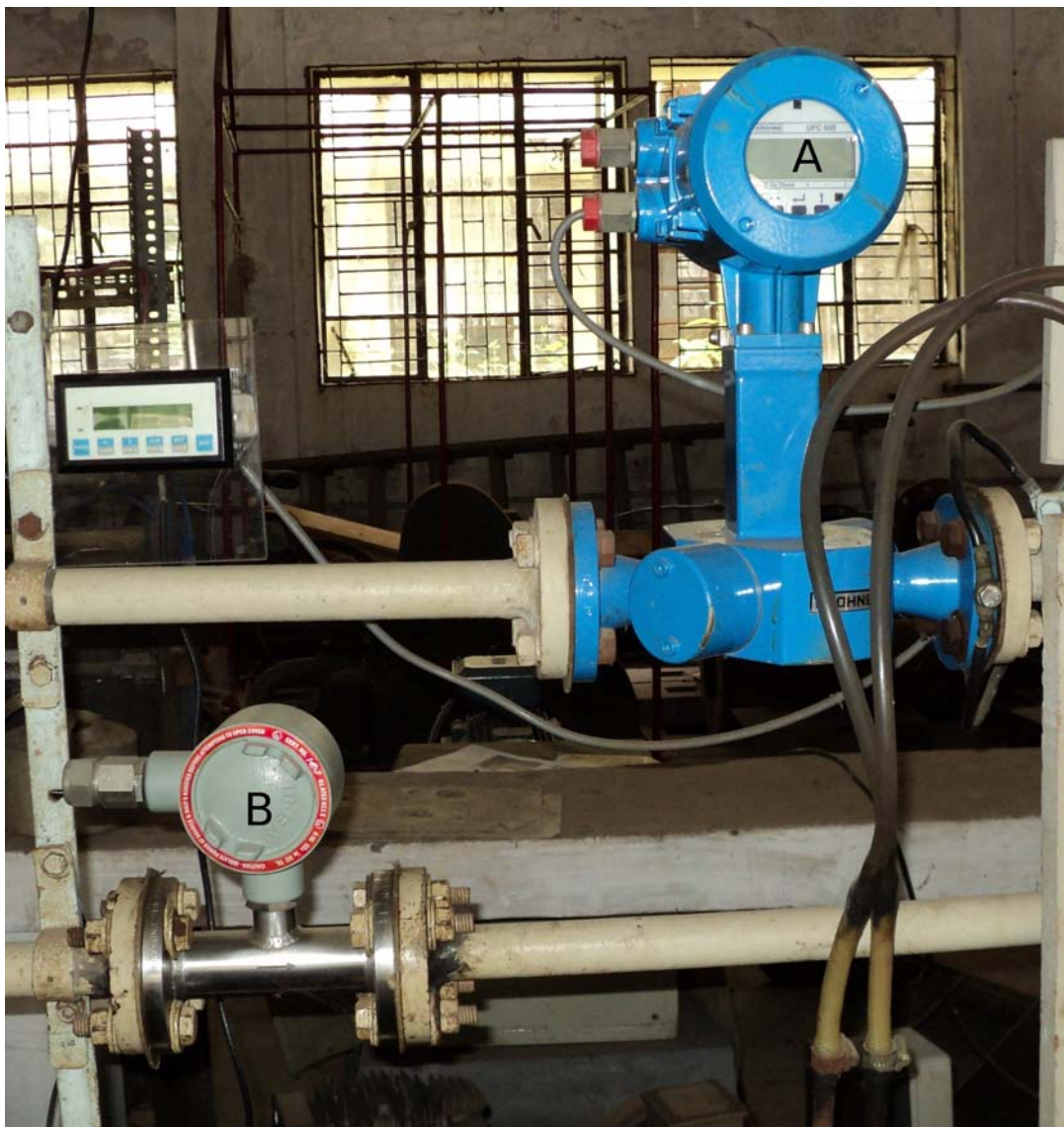


Figure 8: A) Electromagnetic Flow-meter, B) Turbine Meter

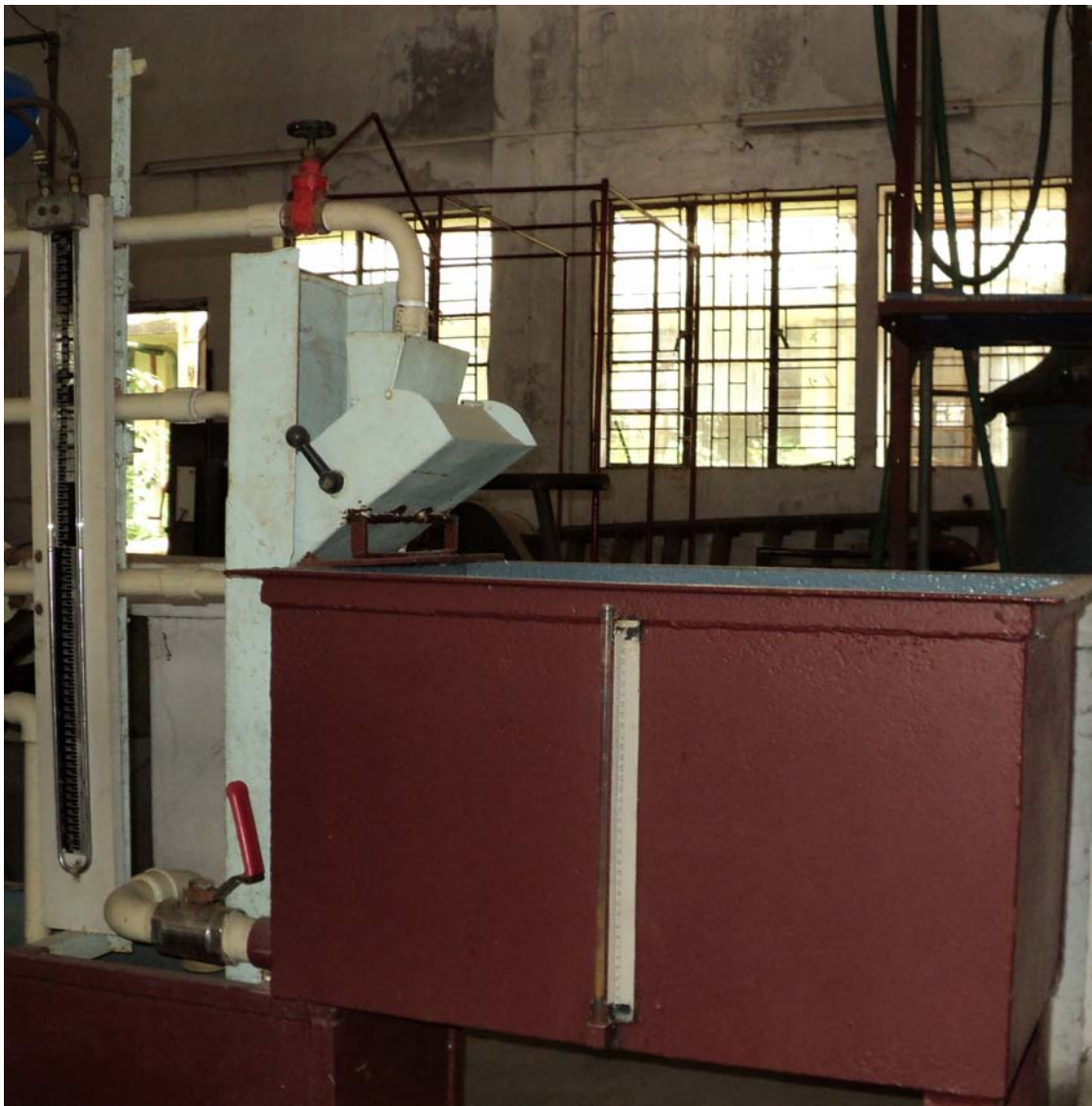


Figure 9: Measuring Tank

# Calibration of an orifice plate by free jet method

Hydraulics Laboratory  
Course: **ME39606**

Department of Mechanical Engineering  
Indian Institute of Technology, Kharagpur

# Calibration of an orifice plate by free jet method

**OBJECTIVE:** To determine  $C_d$  (Coefficient of Discharge) for a circular orifice.

## INSTRUCTIONS:

1. Study the setup and make a line diagram.
2. Fix the head at a certain height.
3. Open the orifice and measure the coordinates of the jet at two different points.
4. Collect the water in the volume measurement tank through the diverter for approximately 3 minutes and note the increase in height of the water level. Calculate the rate of discharge.
5. Repeat steps 2-4 for different values of the head.
6. Calculate  $C_d$  as outlined in the next few pages, assuming that the tank area is  $903\text{cm}^2$  and the orifice diameter is 7.12mm.
7. Plot  $C_d$  versus the Reynolds number  $Re$ .
8. Estimate the uncertainty in the value of  $C_d$ .



(a) Constant head tank



(b) Measurement system

Figure 1: Experimental setup

Let us consider a system where water is issuing out of a reservoir through an orifice plate as shown in Fig. 2.

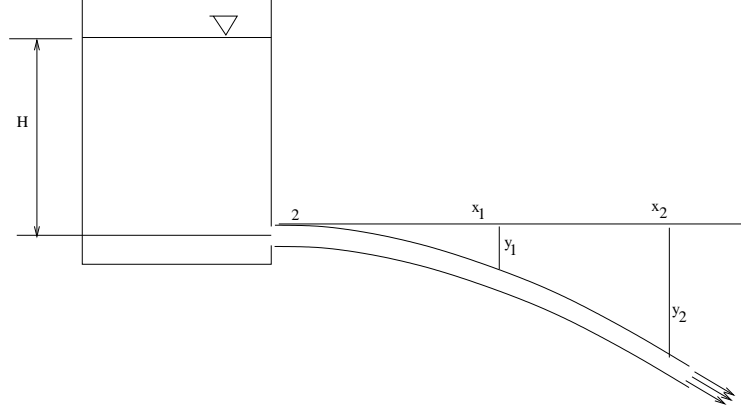


Figure 2: Schematic diagram

As shown in the figure, the constant head maintained is  $H$  such that the theoretical velocity at the orifice outlet is  $V_{th} = \sqrt{2gH}$  [Ex: Derive this expression]. The vena contracta is situated a little away from the orifice plate at point marked 2 and the velocity at vena contracta is defined as  $V_a$ . The cross-section area of orifice plate is  $A_0$  whereas the area of jet at vena contracta is  $A_2$ .

So, velocity coefficient  $C_v$  and the contraction coefficient  $C_c$  are defined as :  $C_v = \frac{V_a}{V_{th}}$  and  $C_c = \frac{A_2}{A_0}$ . The actual discharge is given by  $Q_a = A_2 V_a = A_0 C_c C_v V_{th} = C_d A_0 V_{th}$ . Here, the discharge coefficient  $C_d$  is defined as  $C_d = C_c C_v$ . The discharge coefficient is experimentally found out if  $C_c$  and  $C_v$  are known [Exercise: How will you estimate  $C_c$ ?]

## To obtain $C_v$ :

With reference to Fig. 2, we can measure  $x_1$  and  $y_1$ . We can write  $x_1 = V_a t$  and  $y_1 = \frac{1}{2} g t^2$ . Eliminating  $t$ , we obtain  $V_a = \frac{x_1}{\sqrt{\frac{2y_1}{g}}}$ .

If we measure at two points 1 and 2, we can write:  $x_1 = V_a t_1$  ,  $y_1 = \frac{1}{2} g t_1^2$  and  $x_2 = V_a t_2$  and  $y_1 = \frac{1}{2} g t_2^2$ .

$$y_2 - y_1 = \frac{1}{2} g(t_2^2 - t_1^2) , x_2 - x_1 = V_a(t_2 - t_1) \text{ and } x_2 + x_1 = V_a(t_2 + t_1)$$

$$\text{Therefore, } V_a = \sqrt{\frac{1}{2} g \frac{x_2^2 - x_1^2}{y_2 - y_1}}$$

So,

$$C_v = \frac{V_a}{V_{th}} = \frac{x_1 / \sqrt{\frac{2y_1}{g}}}{\sqrt{2gH}}$$

or

$$C_v = \frac{V_a}{V_{th}} = \frac{\sqrt{\frac{1}{2} g \frac{x_2^2 - x_1^2}{y_2 - y_1}}}{\sqrt{2gH}}$$

**Caution:** Note that there is a zero error in the scale reading of the apparatus. How will you correct for this in your calculations ?

## Uncertainty analysis:

If one carries out a single-variable experiment a large number of times  $n >> 1$ , and each instance is assumed to be an independent experiment, the error will follow a Gaussian (Normal) distribution. However, it is not possible to carry out a large number of experiments because this is time-consuming, so, a confidence level is considered. If it is assumed that the confidence level is  $3\sigma$  (here  $\sigma$  is the standard deviation), then 1 in 300 experiments will be wrong. For  $2\sigma$ , it will be 1 out of 20 experiments and for  $\sigma$  it will be 1 in 3 experiments. Assuming that  $2\sigma$  is an acceptable confidence level, we now discuss the uncertainty. Considering a variable  $R$  with given functional dependence:

$$R = f(x_1, x_2, \dots, x_n) \quad (1)$$

The individual contribution of  $x_1$  to the total error in  $R$  is given by:

$$\delta R = \frac{\partial R}{\partial x_1} \delta x_1 \quad (2)$$

or

$$\frac{\delta R}{R} = \frac{x_1}{R} \frac{\partial R}{\partial x_1} \frac{\delta x_1}{x_1} \quad (3)$$

Defining the uncertainties as  $u_R = \frac{\delta R}{R}$  and  $u_{x_1} = \frac{\delta x_1}{x_1}$ , the root-mean-square uncertainty in  $R$  is given by

$$u_R = \sqrt{\sum_{i=1..n} \left( \frac{x_i}{R} \frac{\partial R}{\partial x_i} u_{x_i} \right)^2} \quad (4)$$

**Example:** Power  $P$  is given by an expression:  $P = EI$ . Here,  $E = 100 \pm 2V$  and  $I = 10 \pm 0.2A$ . So the nominal power  $P_o = 100 \times 10 = 1000W$ . The maximum value is  $102 \times 10.2 = 1040W$ . The minimum result is  $98 \times 9.8 = 960W$ . Applying the above analysis, we get,

$$u_P = \sqrt{\left( \frac{E}{P_o} I \frac{2}{100} \right)^2 + \left( \frac{I}{P_o} E \frac{0.2}{10} \right)^2} \quad (5)$$

which is equal to 2.83%. This is less than the uncertainty value of 5% assumed above.

## To estimate the uncertainty in $C_d$ :

$$C_d = \frac{Q_a}{Q_{th}} \quad (6)$$

where the actual flowrate  $Q_a$  is the water collected per unit time in the tank and  $Q_{th}$  is the theoretically calculated flow-rate. Equation 6 can be written as:

$$C_d = \frac{A_T \times H_T / t}{A_0 \times \sqrt{2gH}} \quad (7)$$

where  $A_T$  and  $H_T$  are the base area and height of the tank for which the water is collected upto a time  $t$ . Then, the uncertainty in measuring  $C_d$  is given by:

$$u_{C_d} = \sqrt{\left( \frac{A_T}{C_d} \frac{\partial C_d}{\partial A_T} u_{A_T} \right)^2 + \left( \frac{H_T}{C_d} \frac{\partial C_d}{\partial H_T} u_{H_T} \right)^2 + \left( \frac{t}{C_d} \frac{\partial C_d}{\partial t} u_t \right)^2 + \left( \frac{A_0}{C_d} \frac{\partial C_d}{\partial A_0} u_{A_0} \right)^2 + \left( \frac{H}{C_d} \frac{\partial C_d}{\partial H} u_H \right)^2} \quad (8)$$

It can be shown that [Exercise]:

$$\frac{A_T}{C_d} \frac{\partial C_d}{\partial A_T} = 1$$

$$\frac{H_T}{C_d} \frac{\partial C_d}{\partial H_T} = 1$$

$$\frac{t}{C_d} \frac{\partial C_d}{\partial t} = -1$$

$$\frac{A_0}{C_d} \frac{\partial C_d}{\partial A_0} = -1$$

$$\frac{H}{C_d} \frac{\partial C_d}{\partial H} = -0.5$$

The uncertainty in measurements of the area, height, time etc. are to be taken as nominal values:

$$A_T = A_{To} \pm 0.1\%$$

$$H_T = H_{To} \pm 0.1\%$$

$$t = t_o \pm 1\%$$

$$A_0 = A_{0o} \pm 0.1\%$$

$$H = H_o \pm 0.1\%$$

Therefore, the uncertainty in measuring  $C_d$  is given by:

$$u_{C_d} = \sqrt{\left(\frac{0.1}{100}\right)^2 + \left(\frac{0.1}{100}\right)^2 + \left(-\frac{1}{100}\right)^2 + \left(-\frac{0.1}{100}\right)^2 + \left(\frac{-0.05}{100}\right)^2} \quad (9)$$

or,

$$u_{C_d} = 0.0102 = 1.02\%$$

## Exercises

1. Figure 3 is a photograph of a non-Newtonian liquid (containing red dye) exiting an orifice. Explain why the diameter of the jet *increases* as it exits the tube, with no perceptible vena contracta ?
2. In Figure 4, the orifice has a well-rounded opening. Explain why there is no vena contracta and find the mass flow rate at the exit of the orifice given the density  $\rho$ , orifice area  $A$  and height of the water level above the orifice  $h$  ?



Figure 3: Die swell of a non-Newtonian liquid

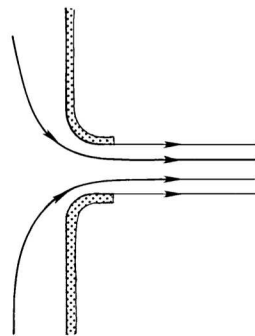


Figure 4: Flow through a rounded orifice